Pergamon

Int. J. Heat Mass Transfer. Vol. 40, No. 8, pp. 1727–1741, 1997

0017-9310/97 $17.00+0.00

PII: S0017-9310(96)00285-2

Efficient computation of particle dispersion in turbulent flows with a stochastic–probabilistic model

X.-Q. CHEN and J. C. F. PEREIRA

Department of Mechanical Engineering, Instituto Superior Técnico/Technical University of Lisbon, Av. Rovisco Pais, 1096 Lisbon Codex, Portugal

(*Received* 12 *March* 1996 *and in final form* 8 *August* 1996)

Abstract—This paper describes a three-dimensional, stochastic–probabilistic, efficiency-enhanced dispersion (SPEED) model for the prediction of particle dispersion in turbulent flows. A stochastic procedure is used to compute particle-trajectory mean and variance, and a probabilistic procedure is used to compute a physical-particle spatial distribution among Eulerian control volumes. An additional Lagrangian equation is derived to govern the evolution of particle-trajectory variance. The SPEED model is aimed at tracking a relatively small number of particle trajectories, while efficiently reducing computational shot noise in the conventional stochastic dispersion model. Two tests cases with available measurements are used to validate the efficiency of the SPEED model. Numerical results of the SPEED model using only 5×10^2 particle trajectories are compared with those of the conventional stochastic model using as high as 1.5×10^4 particle trajectories. It is found that the SPEED model offers better agreement with the experimental measurements, and that the computational efficiency can be substantially enhanced by a factor of 20.

INTRODUCTION

Particle dispersion in turbulent flows finds diverse applications in spray drying, particle classification or removal from fluids and atomized fuel combustion. Most dilute particle-laden turbulent flows are characterized by the presence of a continuous phase and a dispersed phase. For predictions of these dispersed particle-laden turbulent flows, two common approaches are usually employed: Eulerian–Eulerian and Eulerian–Lagrangian. The two approaches differ from each other in the handling of the dispersed phase. The Eulerian–Eulerian approach treats both the continuous and dispersed phases as two interpenetrating continua. For the continuous phase, the existing turbulence closure model for single phase flows can be easily extended to two-phase flows by incorporating some additional coupling sources due to two-phase interactions. Unfortunately, the Eulerian formulation of the dispersed phase can not easily account for the effects of the particle-size spectrum in multisized two-phase flows, let alone account for the trajectory-crossing effects or interparticle collision or coalescence. In contrast, the Lagrangian trajectory model handles discrete particle dispersion using a stochastic method by tracking a large number of individual particle trajectories to achieve a stochastically significant solution. This model is successful in that it tracks the motion of each representative particle parcel; as a result, it is extremely straightforward to account for such effects as particle-size spectrum, crossing trajectories, interparticle coalescence and collisions. Therefore, the Lagrangian treatment of the dispersed phase is receiving more and more attention in predicting dilute two-phase flows.

Since the early work of Yuu *et al.* [1] and Gosman and Ioannides [2], the Lagrangian stochastic model has been widely applied to predict a variety of dilute turbulent two-phase flows. Many encouraging applications have been reported by, among others, Shuen *et al.* [3], Chang and Wu [4], and Berlemont *et al.* [5] for two-dimensional evaporating and nonevaporating two-phase flows. In addition, successful applications of this model to three-dimensional multiphase flows have also been reported by Fiveland and Wessel [6] as well as Coimbra *et al.* [7]. A complete review of the stochastic trajectory model can be found in Faeth [8], Crowe [9], Sirignano [10], and Elghobashi [11], among others. Even though the Lagrangian stochastic model has been successful in predicting various two-phase or multiphase flows, one problem persists due to the stochastic procedure used in the conventional Lagrangian trajectory computations, that is, when a discrete delta-function dispersion is used for the distribution of physical particles. Many authors have found it necessary to track a "large" number of particle trajectories to achieve stochastically significant solutions for two-dimensional flows; see Sturgess *et al.* [12], Mostafa *et al.* [13], Chang and Wu [4], and Chen and Pereira [14]. In these computations, a total number of particle trajectories, ranging from 3×10^3 to 10^5, were used to achieve stochastically significant or invariant solutions. Obviously, for industrial applications where three-dimensional computations are

often encountered, it would be unacceptable, even for present supercomputers, to track such a large number of particle trajectories. Evidently, other alternative models have to be sought to bring the existing Lagrangian stochastic model into industrial applications. These alternative models should keep the advantages of the existing Lagrangian trajectory model but reduce the requirement of tracking a large number of particle trajectories. To this end, Litchford and Jeng [15] developed a stochastic dispersion-width transport model, where the dispersion-width is explicitly computed through the linearized equation of motion using the concept of particle-eddy interactions. The application and subsequent improvement of this model have been made by Chen and Pereira [16] for turbulent evaporating sprays where the effects of turbulence anisotropy and artificial particle drift correction have been taken into account. However, this model has the shortcoming that too many repeated summing operations are required to determine the dispersion-width. Even though this stochastic dispersion-width transport model significantly reduces the number of particle trajectories, it requires many repeated summing operations to compute the dispersion-width, a process which is very time consuming. Moreover, this model considers only the dispersion effects in the cross-streamwise direction and needs a correction constant to account for undersampling. To overcome these shortcomings of the stochastic dispersion-width transport model, the present study is aimed at developing a generalized, three-dimensional, Lagrangian trajectory model which keeps the advantages of the conventional discrete delta-function model but overcomes the deficiency in tracking a "large" number of particle trajectories; therefore, computational efficiency can be substantially increased. The model developed here adopts a combined stochastic-probabilistic method to describe the turbulent motion of discrete particles so that only a small number of particle trajectories are required.

Two test cases of particle-laden turbulent flows are used to validate the developed SPEED model. Numerical predictions are compared with available experimental measurements. The efficiency and accuracy of the model are assessed against the conventional stochastic model and experimental measurements.

STOCHASTIC COMPUTATION OF TRAJECTORY MEAN AND VARIANCE

In the framework of Lagrangian formulation, the equation of motion of each of the representative particle sizes can be written as

$$\frac{\mathrm{d}U_{\mathrm{p}i}}{\mathrm{d}t} = \frac{\tilde{U}_i - U_{\mathrm{p}i}}{\tau_{\mathrm{p}}} + F_{\mathrm{p}i} \tag{1}$$

where the subscript p represents the particle phase, i the Cartesian components, t time, $\tilde{U}_i$ the fluid instantaneous velocity, τ_{p} the particle relaxation time, and $F_{\mathrm{p}i}$ an extra force, such as the lift force or gravity force. Note that the instantaneous velocity consists of two parts: the mean U_i and fluctuating u_i' which is "seen" by a discrete particle. The continuous-phase fluctuating velocity can be determined using an anisotropic particle dispersion model [14], based on the concept of particle-eddy encounters [1, 2]:

$$u_i' = \sqrt{\overline{u_i'^2}}\,\xi_i \tag{2}$$

where ξ_i is a Gaussian random variable having zero mean and unity variance and $\overline{u_i'^2}$ is the continuous-phase normal stress which can be obtained with a turbulence closure model. Note that no summation practice is adopted for repeated subscripts in the present study. The fluctuating velocity given by equation (2) is fixed in equation (1) within the period of time when a particle is interacting with a randomly sampled turbulent eddy. The interaction time is determined by minimizing two time scales of an eddy-life time and eddy-transit time. Details of this particle-eddy encounter model can be found elsewhere [2, 3]. The relaxation time of a particle in equation (1) is defined as

$$\tau_{\mathrm{p}} = \frac{\rho_{\mathrm{p}} D_{\mathrm{p}}^2}{18\mu f_{\mathrm{p}}} \tag{3}$$

where ρ_{p} is the particle density, D_{p} the particle diameter, μ the fluid viscosity, and f_{p} the drag correction coefficient determined by

$$f_{\mathrm{p}} = 1 + 0.15 Re_{\mathrm{p}}^{0.687} \quad (0 < Re_{\mathrm{p}} < 1000). \tag{4}$$

The relative Reynolds number is defined as

$$Re_{\mathrm{p}} = \frac{\rho V_{\mathrm{r}} D_{\mathrm{p}}}{\mu} \tag{5}$$

where ρ is the fluid density and V_{r} is the relative velocity between the two phases, given by

$$V_{\mathrm{r}} = \sqrt{\Sigma (U_{\mathrm{p}i} - \tilde{U}_i)^2}. \tag{6}$$

With available particle velocities, it suffices to determine its trajectories by

$$x_{\mathrm{p}i}(t) = x_{\mathrm{p}i}(0) + \int_0^t U_{\mathrm{p}i}(t_1)\mathrm{d}t_1 \tag{7}$$

where $x_{\mathrm{p}i}(0)$ denotes the initial particle position at the inlet. In conventional Lagrangian stochastic dispersion models, computed particle trajectories only represent a single point in space corresponding to the current particle position. In other words, a discrete delta-function distribution is employed as the spatial distribution of a particle variable,

$$\phi(\mathbf{x}) = \phi(\mathbf{x}_{\mathrm{p}})\delta(\mathbf{x} - \mathbf{x}_{\mathrm{p}}) \tag{8}$$

where the vector is used here to represent the three components for conciseness. Therefore, the distribution characterised by equation (8) often requires tracking a relatively large number of particle tra-

jectories to achieve a stochastically significant solution; otherwise, numerical shot-noise occurs in predicted particle properties. As a result, two-way coupling sources also suffer from this kind of numerical shot-noise. The discontinuity or sudden change in two-way coupling sources due to the small number of particle trajectories will unfavourably affect the convergence rate of the overall two-phase iterative solution. This is particularly true of relatively dense two-phase flows, where two-way coupling effects are pronounced. Hence, no matter whether it is from the point of view of stochastic significance or from the point of view of the overall fast convergence rate, the conventional stochastic dispersion model is hopelessly inefficient for tracking a relatively large number of particle trajectories. The root cause necessitating a large number of particle trajectories originates from the method used to estimate particle properties and two-way coupling sources, that is, the use of a discrete delta-function distribution in Lagrangian computations. To overcome the deficiency in conventional Lagrangian stochastic models, a stochastic-probabilistic efficiency-enhanced dispersion (SPEED) model is developed in the present study. In the SPEED model, a conventional Lagrangian stochastic model is first used to determine particle-trajectory mean values, and then a probabilistic method is employed to give the spatial distribution of physical properties in terms of a computed particle dispersion variance. The probabilistic distribution is governed by a prescribed probability density function (PDF). This combined stochastic-probabilistic computation can enhance computational efficiency in that it requires tracking a relatively few number of particle trajectories while efficiently reducing numerical shot-noise, which is often present in conventional, solely-stochastic dispersion models. Now, the problem is hinged upon the determination of particle dispersion variance at each Lagrangian time step. In what follows is the derivation of an ordinary-differential equation to be used for governing the evolution of particle dispersion variance along its trajectory.

Suppose that at each time step a particle-trajectory fluctuation due to fluid turbulence is x'_{pi}, whose mean value is x_{pi} is given by equation (7). Obviously, the particle-trajectory variance is x'^2_{pi}, whose derivative with respect to time yields

$$\frac{dx'^2_{pi}}{dt} = 2x'_{pi}\frac{dx'_{pi}}{dt} = 2x'_{pi}u'_{pi} \tag{9}$$

where u'_{pi} represents the particle velocity fluctuation. x'_{pi} can be determined by integrating u'_{pi} over time

$$x'_{pi} = \int_0^t u'_{pi}(t_1)dt_1. \tag{10}$$

The derivation of equation (10) is detailed in Appendix A. Introducing equation (10) into equation (9) and ensemble-averaging it over a large number of samples, we have

$$\frac{d\langle x'^2_{pi}\rangle}{dt} = 2\int_0^t \langle u'_{pi}(t)u'_{pi}(t_1)\rangle dt_1 \tag{11}$$

where $\langle\rangle$ denotes an ensemble-averaging process, and $\langle u'_{pi}(t)u'_{pi}(t_1)\rangle$ represents the correlation of particle velocity fluctuations between the time interval of t and t_1. Evidently, no direct information is available for this particle-velocity correlation along its trajectory. However, the use of a turbulence closure model (namely, the Reynolds-stress model) can provide us with the predicted Reynolds stresses of the continuous phase, even though particle velocity fluctuations usually do not follow those of its carrier phase. Therefore, an expression may be derived to relate the velocity-fluctuations of the particle phase to the fluid phase; that is

$$\langle u'_{pi}(t)u'_{pi}(t_1)\rangle = \Omega_p\langle u'_i(t)u'_i(t_1)\rangle \tag{12}$$

where $\langle u'_i(t)u'_i(t_1)\rangle$ represents the correlation of the velocity fluctuations for fluid tracers and Ω_p accounts for the slipping effects between the two phases. In the twin-fluid modeling of particle-laden turbulent flows, a similar problem exists for the modeling of particle turbulent viscosity [17, 18]. Similarly, it follows that

$$\Omega_p = \begin{cases} \dfrac{1}{1+St} & \text{Model A} \\ \sigma_p\left[1+3C_\beta\dfrac{V_r^2}{2k}\right]^{-1/2} & \text{Model B} \end{cases} \tag{13}$$

where Models A and B have been, respectively, employed by Rizk and Elghobashi [17] and Adeniji-Fashola and Chen [18] to determine particle turbulent viscosity in the twin-fluid model. The model constants in equation (13) are $\sigma_p = 1.5$ and $C_\beta = 0.85$. The Stokes number, St, is defined as the ratio of the particle relaxation timescale, τ_p, to the characteristic timescale of the flow τ_f, that is,

$$St = \frac{\tau_p}{\tau_f} \tag{14}$$

where τ_p is given by equation (3). The physical background for Model A can be easily examined when a particle approaches to a tracer limit. In this context, the Stokes number becomes very small and the particle will totally follow the fluid motion; as a result, the particle fluctuating velocity variance should approach that of the fluid tracers. However, the effect of the Stokes number on Model B is implicitly accounted for through the relative velocity between the two phases. Detailed discussion of this model can be found in Picart *et al.* [19]. To determine the fluid velocity correlation, a Lagrangian autocorrelation function, $R_{Li}(\tau)$, is used. It is defined as

$$R_{Li}(\tau) = \frac{\langle u'_i(t)u'_i(t+\tau)\rangle}{\langle u'^2_i(t)\rangle} \tag{15}$$

where $\tau = t_1 - t$. Following Berlemont *et al.* [20] and Zhou and Leschziner [21], we employ a Frenkiel cor-

relation function to determine the autocorrelation function by

$$R_{Li}(\tau) = \cos\left(\frac{\tau}{2T_{Li}}\right)\exp\left(-\frac{\tau}{2T_{Li}}\right) \tag{16}$$

where the integral time scale for each component is determined by

$$T_{Li} = 0.235\frac{\langle u_i'^2(t)\rangle}{\varepsilon} \tag{17}$$

with ε being the dissipation rate of the turbulent kinetic energy, k. When the k-ε model is used, usually no reliable information is available for the anisotropy of turbulence; under these circumstances, the autocorrelation function can be simply determined by

$$R_{Li}(\tau) = R_L(\tau) = \exp\left(-\frac{\tau}{T_L}\right) \tag{18}$$

where T_L is a Lagrangian integral timescale, given by $T_L = 0.3\,k/\varepsilon$. Introducing equation (15) into equation (11), we finally obtain an equation governing the dispersion variance of the particle trajectory,

$$\frac{\mathrm{d}\langle x_{pi}'^2\rangle}{\mathrm{d}t} = 2\Omega_p\langle u_i'^2(t)\rangle\int_0^t R_{Li}(\tau)\mathrm{d}\tau \tag{19}$$

which can be integrated, using available continuous-phase flow properties, to give the evolution of the particle-trajectory variance. This is the fundamental equation sought for the SPEED model to determine the particle trajectory variance at each Lagrangian integral time step.

PROBABILISTIC COMPUTATION OF PARTICLE SPATIAL DISTRIBUTION

It now becomes possible to determine both the particle-trajectory mean value, x_{pi}, and its variance, $\langle x_{pi}'^2\rangle$. The determination of the variance is aimed at providing a spatial distribution, instead of only a single point delta-function distribution, as described by equation (8). To perform the spatial distribution, it is necessary to prescribe a PDF, $f(\mathbf{x})$, which is naturally not known *a priori*. This will be discussed later. With a given PDF of $f(\mathbf{x})$, the spatial distribution of $\phi(\mathbf{x}_p)$, which is computed at the current mean particle position, $\mathbf{x}_p$, is given by

$$\phi(\mathbf{x}) = \int\langle\phi(\mathbf{x}_p)\rangle f(\mathbf{x})\mathrm{d}\mathbf{x} \tag{20}$$

where the integral is performed over an Eulerian control volume. Note that $\langle\phi(\mathbf{x}_p)\rangle$ refers to a particle property which is obtained by ensemble averaging of all individual particle trajectories crossing the Eulerian control volume. Therefore,

$$\phi(\mathbf{x}) = \frac{\sum_{k=1}^{M}\dot{N}_k\Delta t_k\int\phi_k(\mathbf{x}_p)f_k(\mathbf{x})\mathrm{d}\mathbf{x}}{\sum_{k=1}^{M}\dot{N}_k\Delta t_k\int f_k(\mathbf{x})\mathrm{d}\mathbf{x}} \tag{21}$$

where the summation over k represents all the particle sizes crossing the Eulerian control volume with M being the total number of the particle trajectories. $\dot{N}_k$ in equation (21) denotes the particle number flowrate of the kth particle, and the product of $\dot{N}_k$ and Δt_k stands for the total number of particles in the Eulerian control volume in question. Of note is that the spatial distribution given by equation (21) is only valid for particle number-ensembled properties. For the two-way coupling source, however, its spatial distribution is given by

$$S_\phi^p(\mathbf{x}) = \sum_{k=1}^{M}\dot{N}_k\Delta t_k\int S_{\phi_k}^p(\mathbf{x}_p)f_k(\mathbf{x})\mathrm{d}\mathbf{x} \tag{22}$$

where $S_{\phi_k}^p$ is determined in Lagrangian-trajectory computations in terms of the two-way coupling expressions [14, 22].

It is now clear that the spatial distribution of a particle property of a two-way coupling source can be easily carried out with resort to equations (21) and (22), if the probability density function, $f(\mathbf{x})$, has been prescribed or is experimentally known. In their sensitivity study of various PDF shapes on a dispersion-width transport model, Litchford and Jeng [23] found that given an appropriate dispersion-width, the particle spatial distribution is not very sensitive to the shape of the PDF, and that slightly better results are achieved with a Gaussian PDF. Therefore, the Gaussian distribution is used. Expressed as a product of its three components, the three-dimensional Gaussian PDF can be written as

$$f(\mathbf{x}) = \prod_{i=1}^{3}\frac{1}{\sqrt{2\pi}\sigma_{pi}}\exp\left[-\frac{(x_i - x_{pi})^2}{2\sigma_{pi}^2}\right] \tag{23}$$

where σ_{pi} is the standard deviation of the particle trajectory fluctuations, given by

$$\sigma_{pi} = \langle x_{pi}'^2\rangle^{1/2}. \tag{24}$$

In accordance with its definition, the probability distribution function of the i-component reads

$$F(x_i) = \int_{-\infty}^{x_i} f(x_i)\mathrm{d}x_i = \int_{-\infty}^{x_i}\frac{1}{\sqrt{2\pi}\sigma_{pi}}\exp\left[-\frac{(x_i - x_{pi})^2}{2\sigma_{pi}^2}\right]\mathrm{d}x_i \tag{25}$$

from which the three-dimensional probability distribution function can be determined. Hence, the spatial distribution of an ensemble-averaged particle property can be rewritten as

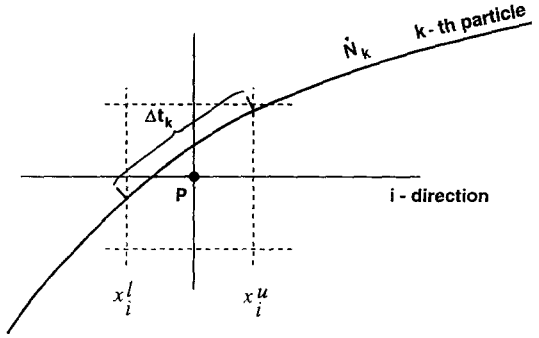

Fig. 1. Definition of the integral boundaries.

$$\phi(\mathbf{x}) = \frac{\sum_{k=1}^{M} \dot{N}_k \Delta t_k \int_{x_1^l}^{x_1^u} \int_{x_2^l}^{x_2^u} \int_{x_3^l}^{x_3^u} \phi_k(x_{p1}, x_{p2}, x_{p3}) \times f_k(x_1, x_2, x_3) \mathrm{d}x_1 \mathrm{d}x_2 \mathrm{d}x_3}{\sum_{k=1}^{M} \dot{N}_k \Delta t_k \int_{x_1^l}^{x_1^u} \int_{x_2^l}^{x_2^u} \int_{x_3^l}^{x_3^u} f_k(x_1, x_2, x_3) \mathrm{d}x_1 \mathrm{d}x_2 \mathrm{d}x_3} \tag{26}$$

where the superscripts l and u represent the lower and upper boundaries of an Eulerian control volume along the i-direction, respectively, as shown in Fig. 1. Introduction of the probability distribution function of equation (25) into equation (26) leads to

$$\phi(\mathbf{x}) = \frac{\sum_{k=1}^{M} \dot{N}_k \Delta t_k \phi_k(\mathbf{x}_p) \left\{ \prod_{i=1}^{3} [F_k(x_i^u) - F_k(x_i^l)] \right\}}{\sum_{k=1}^{M} \dot{N}_k \Delta t_k \left\{ \prod_{i=1}^{3} [F_k(x_i^u) - F_k(x_i^l)] \right\}}. \tag{27}$$

Similarly, the spatial distribution of equation (22) for the two-way coupling source can be rewritten as

$$S_\phi^p(\mathbf{x}) = \sum_{k=1}^{M} \dot{N}_k \Delta t_k S_{\phi_k}^p(\mathbf{x}_p) \left\{ \prod_{i=1}^{3} [F_k(x_i^u) - F_k(x_i^l)] \right\}. \tag{28}$$

Of particular note is that the afore-described spatial distributions have not accounted for the presence of the physical boundaries, which often exist in confined particle-laden turbulent flows. To take into account the presence of the physical domain, the probability distribution function has to be normalized to satisfy the requirement that the integral over the physical domain is equal to unity, i.e.

$$P(x_i) = \frac{F(x_i)}{F(x_i^{\max}) - F(x_i^{\min})} \tag{29}$$

where $x_i^{\max}$ and $x_i^{\min}$ are, respectively, the two physical boundaries corresponding to the i-direction. Therefore, $P(x_i)$ should be used to substitute $F(x_i)$ in equations (27) and (28) to account for the presence of the physical boundaries. Of course, for problems where near-wall particle deposition and reflection are important, appropriate particle-deposition and particle-wall interaction models are necessarily employed. Such a physical phenomenon can be accounted for by incorporating into the SPEED model adequate particle-deposition and particle-wall interaction models.

MISCELLANEOUS REMARKS

When computing the spatial distribution of a physical particle, the probability distribution function shape is necessarily assumed for each component; see equation (25). Following Abramowitz and Stegun [24], equation (25) can be estimated by

$$F(x_i) = 1 - f(\lambda_i) \sum_{n=1}^{5} \beta_n \zeta^n \tag{30}$$

where λ_i is defined as

$$\lambda_i = \frac{x_i - x_{pi}}{\sigma_{pi}} \tag{31}$$

and ζ is defined as

$$\zeta = \frac{1}{1 + \beta_0 \lambda_i}. \tag{32}$$

The coefficients in equations (30) and (32) are listed in Table 1. Therefore, the probability distribution function can be easily determined with equations (30)–(32) for each component. To enhance computational efficiency, the distance along each direction can be shortened according to the computed dispersion deviations, σ_{pi}. Usually a distance of three times as much as σ_{pi}, i.e. $|\lambda_i| = 3$, suffices to estimate the integration of equation (25). Finally, the overall solution procedure for the SPEED model to compute particle-laden turbulent flows can be outlined as follows:

(i) To set to zero all two-way coupling sources in the continuous-phase Eulerian equations.
(ii) To solve the Eulerian equations for the continuous phase with coupling sources from the Lagrangian trajectory model.
(iii) To perform Lagrangian trajectory computations for particle-trajectory mean and variance, particle number-ensembled properties and two-way coupling sources.
(iv) To distribute the two-way coupling sources in space into Eulerian control volumes for the continuous phase.
(v) To repeat step (ii) to step (iv) until it is converged.

It should be noted that one of the flow configurations widely encountered in engineering applications is characteristic of flow axisymmetry. To refine the numerical grid, the cylindrical coordinates are often used. In such a case, some special care should be taken in determining the spatial distribution, which becomes two-dimensional in cylindrical coordinates even though the flow is still three-dimensional in Cartesian

Table 1. Coefficients of estimating probability distribution function

β_0	β_1	β_2	β_3	β_4	β_5
0.2316419	0.31938153	−0.35656378	1.78417794	−1.82125598	1.33027443

coordinates. The evaluation of the probability distribution function for axisymmetric flow configurations was described elsewhere [16].

NUMERICAL RESULTS AND DISCUSSION

To validate the developed SPEED model, two test cases are considered: dispersion of monosized particles in a plane mixing layer and in a plane coflowing jet. These two tests cases were selected due to the fact that both of them have planar flow configurations and experimental measurements are available; therefore, the present generalized model in Cartesian coordinates can be directly validated. The flow configurations are shown in Fig. 2(a,b).

Test case 1 : *particle dispersion in a planar mixing layer*

The flow configuration is shown in Fig. 2 (a). Detailed experimental measurements were performed by Hishida *et al.* [25]. The experimental data corresponding to the gas-phase velocities of $U_1 = 13.1$ m s^{-1} and $U_2 = 4.0$ m s^{-1} and to the particle diameter of 42 μm are chosen for the numerical calculations. The mass loading ratio of particles to gas in this two-phase flow is extremely small; therefore, only one-way coupling is necessarily considered. As a result, the two-way coupling effects can be isolated from the SPEED model. Several conventional Lagrangian stochastic dispersion models have been comparatively investigated by Chen and Pereira [26], where emphasis was placed on the behavior of different particle dispersion models. The continuous gas-phase turbulence is modeled using a standard k-ε eddy-viscosity model. As can be seen in Fig. 3(a–c), this model can satisfactorily predict the axial mean and fluctuating velocities, except that the transverse fluctuating velocity is overpredicted at the low velocity side and underpredicted at the high velocity side close to the centre of mixing layer downstream of $X = 150$ mm. In general, the numerical predictions agree reasonably well with the experimental measurements of Hishida *et al.* [25].

It is widely recognized that the conventional stochastic discrete delta-function (SDDF) model usually requires tracking a relatively large number of particle trajectories. To see the effects of the number of trajectories on predicted particle property, Fig. 4(a–c) compares two results obtained with the SDDF model using two different numbers of trajectories (5×10^2 vs 1.5×10^4). It is evident that the particle fluctuating velocities are very sensitive to trajectory numbers. However, the particle axial mean velocity is relatively insensitive to the number of particle trajectories. This kind of sensitivity behavior agrees with our previous conclusions drawn for turbulent evaporating sprays [14]. It is obvious that the stochastically significant solution can only be represented by the SDDF results using a total number of 1.5×10^4 trajectories. For the sake of convenience, the following SPEED predications using model A and model B in equation (13) are referred to as the SPEED-A and SPEED-B predictions, respectively.

As stated in the Introduction, the aim of the present study is mainly focused on improving numerical efficiency by using a relatively few particle trajectories in a Lagrangian-trajectory model. Shown in Fig. 5(a–c) are the profiles of predicted and measured particle mean and fluctuating velocities at the five measured stations of $X = 50$, 100, 150, 200 and 250 mm. Note that substantially different numbers of particle trajectories are employed for the SPEED and SDDF models. The SPEED model computes only a total number of 5×10^2 trajectories whereas the SDDF model computes a total number of 1.5×10^4 trajectories. In general, the SPEED-A and SDDF predictions are agreeable with each other, regardless of the large difference in trajectory numbers tracked in these two models. Note that the profiles of the particle mean and fluctuating velocities obtained with the SPEED-B are also compared with the SDDF model in these figures. It is clearly evident that the SPEED-B predictions are much smoother than the SPEED-A predictions. However, the particle axial mean velocity is slightly overpredicted at the low-velocity side and underpredicted at the high-velocity side, which is closely associated with the predicted gas-phase transverse fluctuating velocity; see Fig. 3(c). Even though this tendency can also be observed in the SPEED-A predictions downstream of $X = 200$ mm, the extent is smaller than the SPEED-B. This may be attributed to the fact that inclusion of a Stokes number, St, in model A can damp out the overpredicted gas-phase transverse fluctuating velocity. In addition, it may not be appropriate to assess the present model using the plane mixing layer which is characterized by large organized structures; see Crowe *et al.* [27]. However, from the point of view of numerical efficiency, the SPEED model does require tracking only a very few number of particle trajectories while yielding very smooth profiles. To more adequately validate the developed SPEED model, the second test case of a

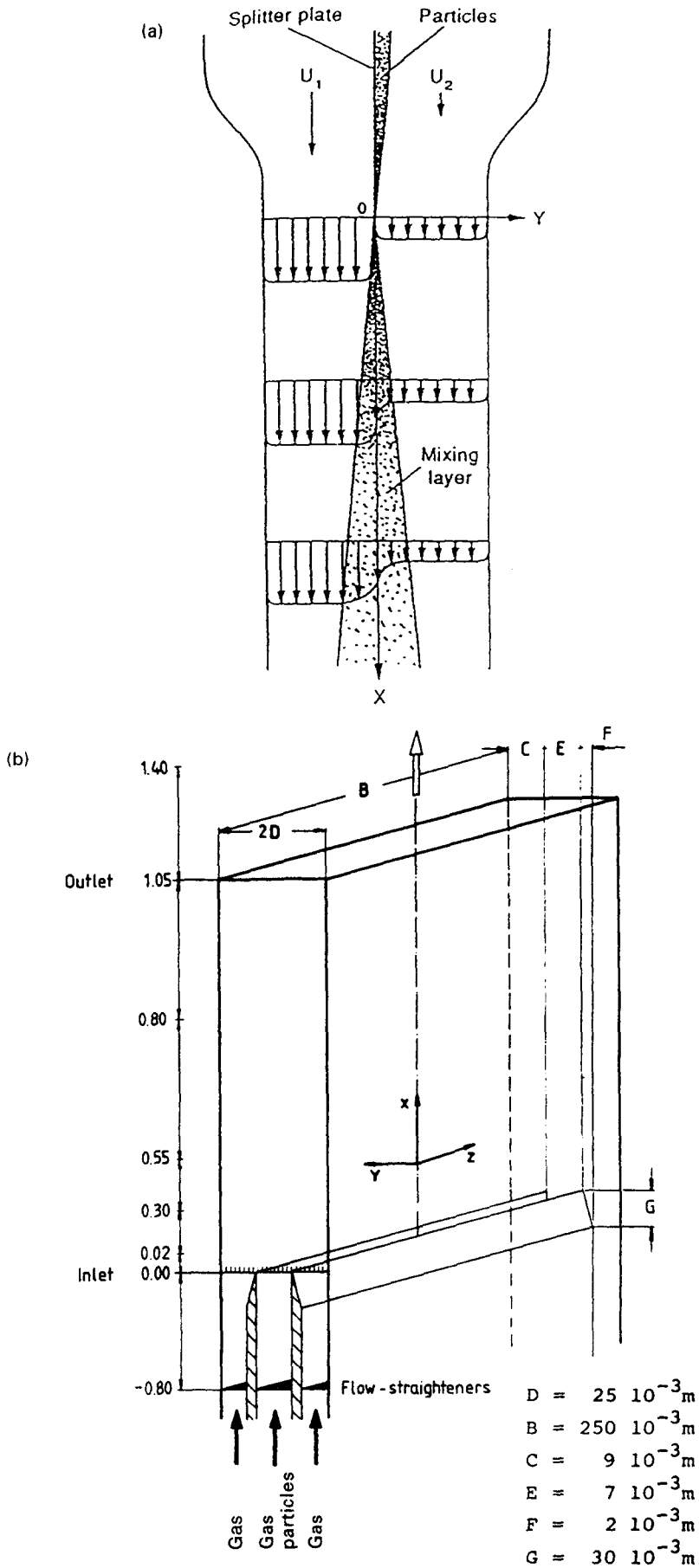

Fig. 2. Flow configurations: (a) plane mixing layer; (b) plane coflowing jet.

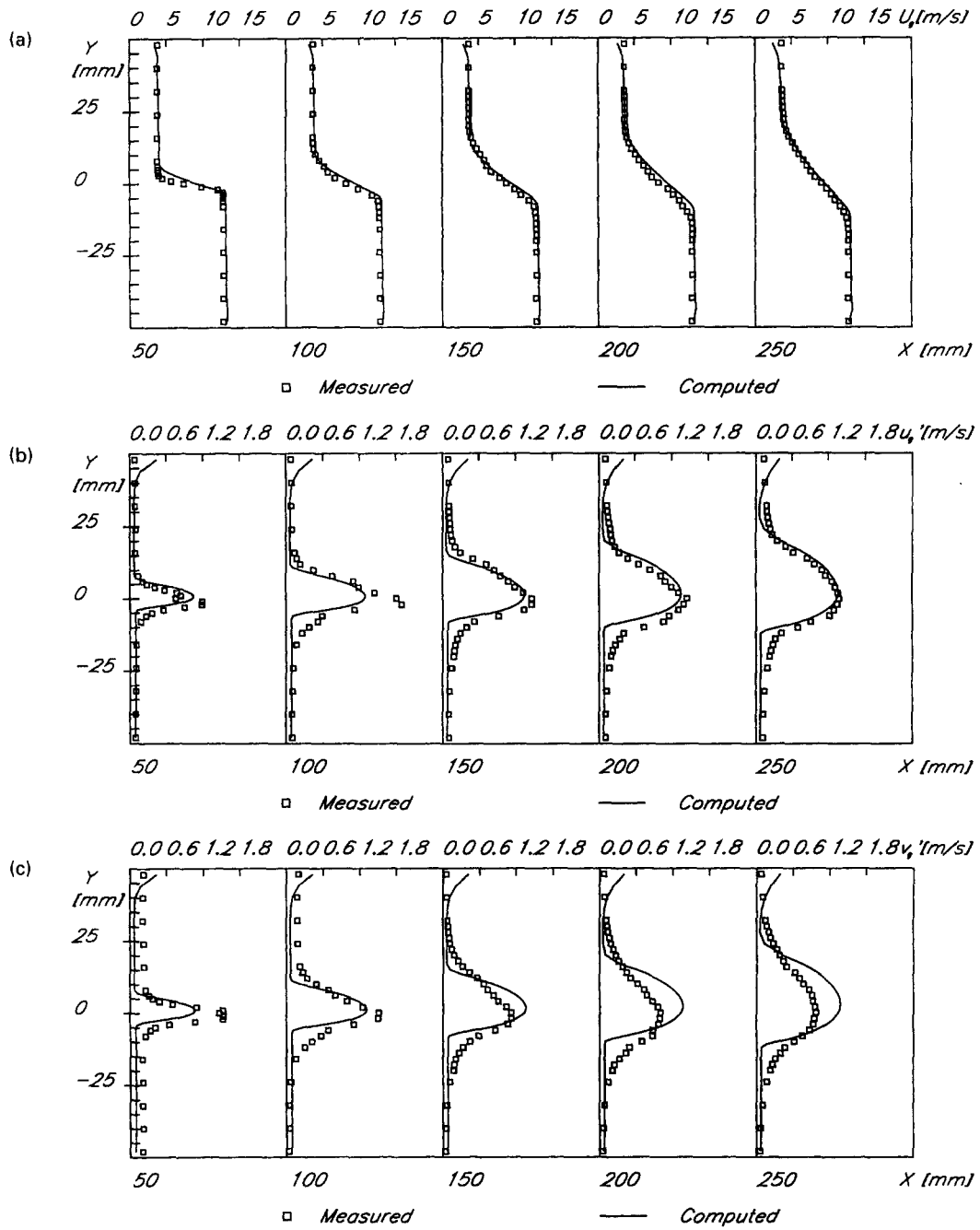

Fig. 3. Comparison of gas-phase velocity profiles: (a) axial mean; (b) axial r.m.s.; (c) transverse r.m.s.

particle-laden turbulent coflowing jet is further investigated.

Test case 2: *particle dispersion in a coflowing planar jet*

The flow configuration is shown in Fig. 2(b). Detailed descriptions of the test case can be found elsewhere [28, 29]. The experimental measurements were reported by Borner *et al.* [30]. The central jet for the test case has a mean velocity of 10.75 m s^{-1} for the gas phase and 9.27 m s^{-1} for the particle phase. The mean velocity of the coflowing airstream around the central jet is 8.2 m s^{-1}. The average particle diameter is 108 μm. To focus on the comparison of trajectory-model efficiency of the particle phase, only a simplified particle-wall interaction model [28] is employed.

Figure 6(a,b) show, respectively, the predicted and measured profiles of the axial mean and fluctuating velocities of the gas phase. It can be seen that the predictions agree well with the measurements.

To see the effects of the number of particle trajectories on particle properties, Fig. 7(a–c) compares two results obtained with the SDDF model using two

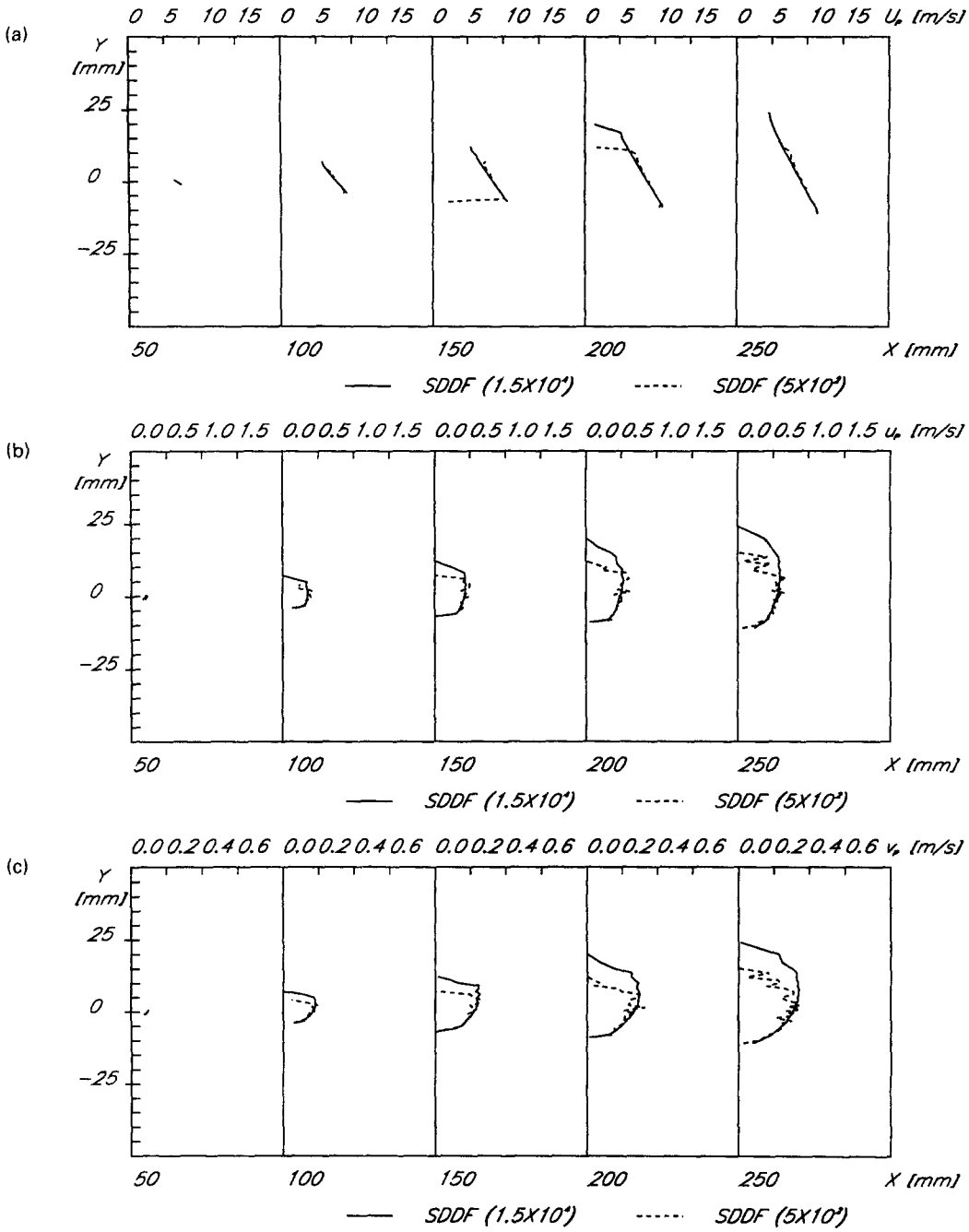

Fig. 4. SDDF predictions of particle-phase velocity profiles obtained using 5×10^2 and 1.5×10^4 trajectories: (a) axial mean; (b) axial r.m.s.; (c) transverse r.m.s.

different numbers of particle trajectories (5×10^2 vs 1.5×10^4). Once again, it is found that the particle axial mean velocity is not very sensitive to the number of trajectories. However, its fluctuating velocity and volume concentration are particularly sensitive to the number of trajectories. Obviously, only the results obtained using a total number of 1.5×10^4 trajectories can be regarded as a stochastically significant solution and are used for the ensuing discussion. To further assess the two suggested expressions relating the particle to gas velocity fluctuations in equation (13), the two SPEED model predictions are compared with those of the SDDF model.

Shown in Fig. 8(a–c) are the profiles of the axial mean velocity, axial fluctuating velocity, and volume concentration of the particle phase obtained with the SPEED and SDDF models. These figures demonstrate that the SPEED models can generally achieve comparably smooth results as compared with the SDDF model, even though the former computes a much smaller number of particle trajectories. Note that both SPEED-A and SDDF models underpredict

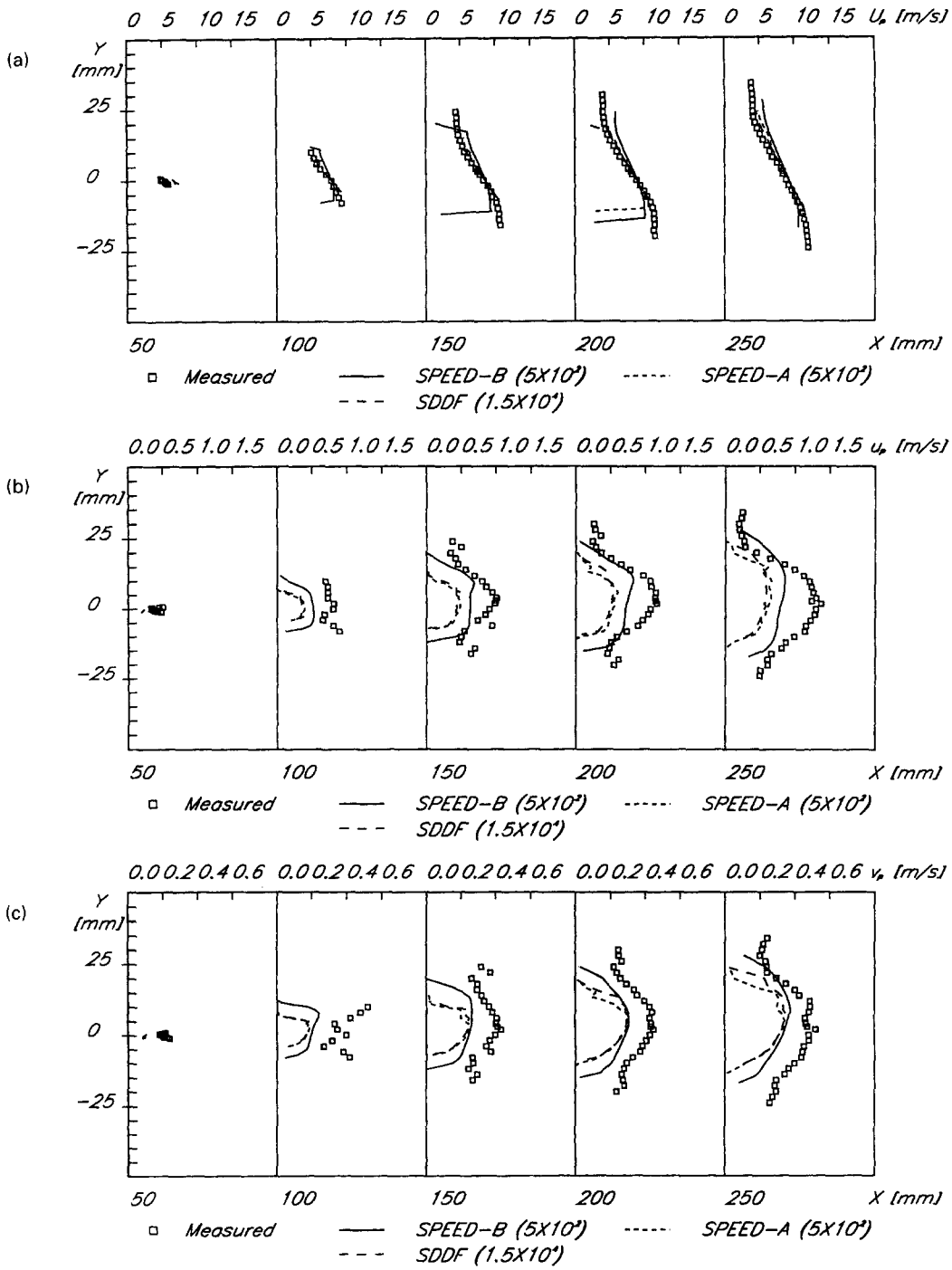

Fig. 5. Predictions of particle-phase velocity profiles with SPEED-A and SPEED-B (5×10^2) as well as SDDF (1.5×10^4): (a) axial mean; (b) axial r.m.s.; (c) transverse r.m.s.

the particle fluctuating velocity far downstream, and have irregular behavior of predicted volume concentration close to the wall, which has also been observed by Azevedo and Pereira [28]. However, these profiles have been much improved with the SPEED-B model. It is found, surprisingly, that the SPEED-B yields much better predictions of particle fluctuating velocity and volume concentration than the SDDF model. Of particular interest is that the curvature of the particle volume concentration, downstream of $X = 550$ mm, is well predicted with the SPEED-B model, and is in very good accord with that of the measurement. Moreover, near-wall irregular behavior is no longer observed in the SPEED-B predictions. This clearly demonstrates that the SPEED-B model can not only give smooth profiles with a very small number of particle trajectories, but also yield more agreeable results with experimental measurements.

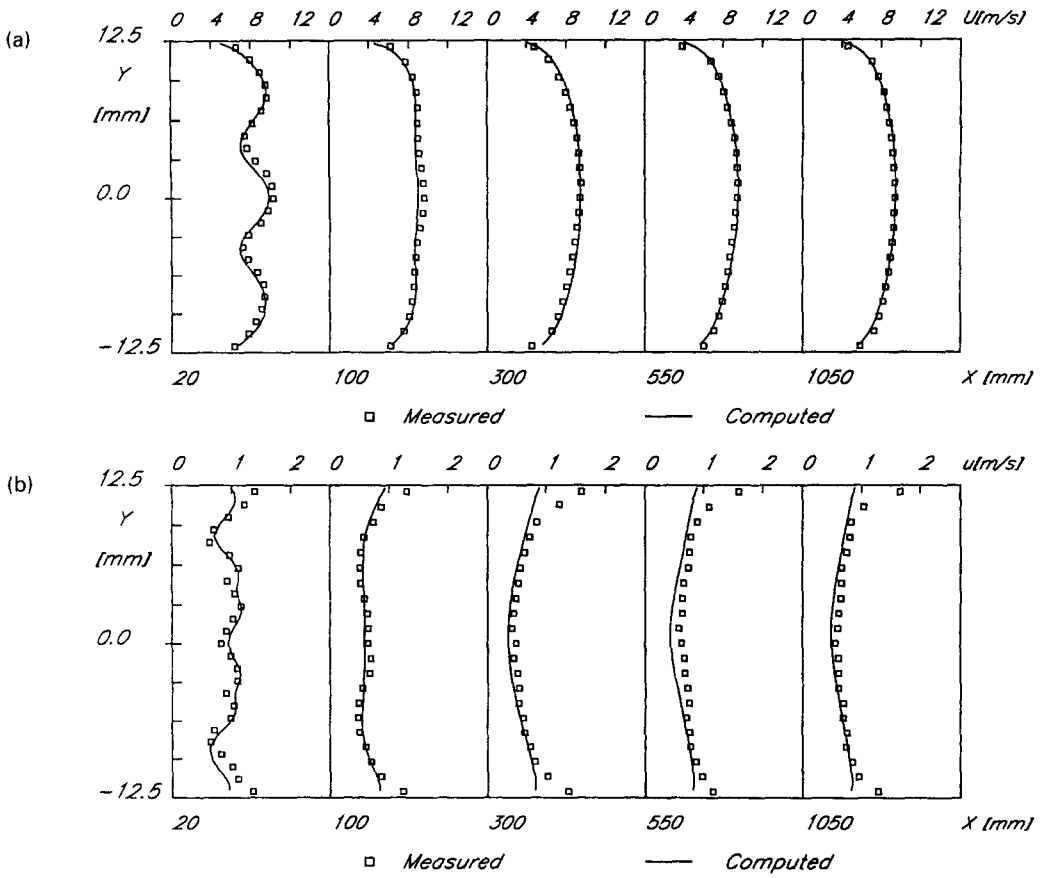

Fig. 6. Comparison of gas-phase velocity profiles: (a) axial mean; (b) axial r.m.s.

Last, but not of least importance, the efficiency of the SPEED and SDDF models is examined in terms of the CPU time consumed in each model computation. The computations were performed with a DEC Alpha 7610 computer at IST, Lisbon. It is found that the SPEED model requires about 1.5 and 1.7 min of CPU time to perform each Lagrangian tracking of 5×10^2 particle trajectories for test case 1 and test case 2, respectively, while the SDDF model requires about 27.2 and 30.6 min of CPU time for each tracking of 1.5×10^4 trajectories for test case 1 and test case 2, respectively. Even though the absolute CPU time depends on the integral time step and the computational domain used, the ratio of the CPU time spent by the SPEED model to that spent by the SDDF model is clearly demonstrative of the higher computational efficiency gained with the SPEED model. In addition, it is also found that a fewer number of two-way coupling iterations are necessary for test case 2 to achieve final convergence with the SPEED model as compared to the SDDF model. This is because the SPEED model distributes the sources in terms of the probability distribution, thus yielding smooth source distribution in Eulerian equations. As a result, the convergence rate of two-phase iterations can be sped up. It can be inferred that such an advantage of the SPEED model should be very helpful for predicting relatively dense two-phase flows, where two-way coupling effects are pronounced.

CONCLUDING REMARKS

An efficient Lagrangian trajectory model (SPEED) was developed for computation of particle dispersion in turbulent flows. The SPEED model requires tracking a relatively few number of particle trajectories, while a noise-free computational solution can be achieved by spatially distributing the physical particles over the Eulerian control volumes in terms of a Lagrangian probabilistic computation. The spatial distribution is controlled by a dispersion variance, which is, in turn, governed by its own ordinary-differential equation. The SPEED model was validated against two test cases of particle-laden turbulent flows with available experimental measurements. It is found that the SPEED model can substantially enhance the computational efficiency by a factor of 20, owing to the small number of particle trajectories required. Therefore, the SPEED model should become a promising tool for efficient predictions of particle dispersion in turbulent flows of engineering significance.

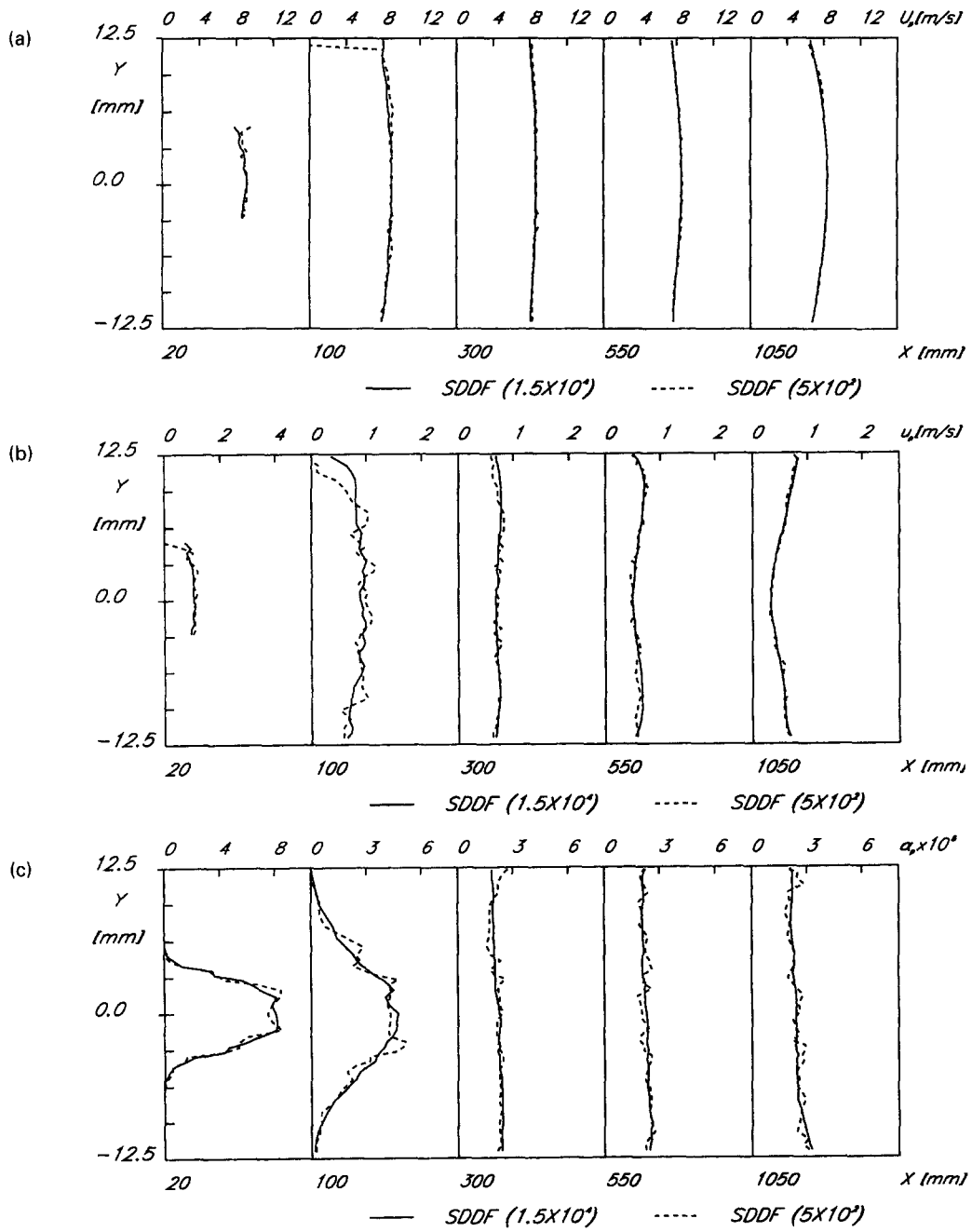

Fig. 7. SDDF predictions of particle-phase properties obtained using 5×10^2 and 1.5×10^4 trajectories: (a) axial mean velocity; (b) axial r.m.s. velocity; (c) volume concentration.

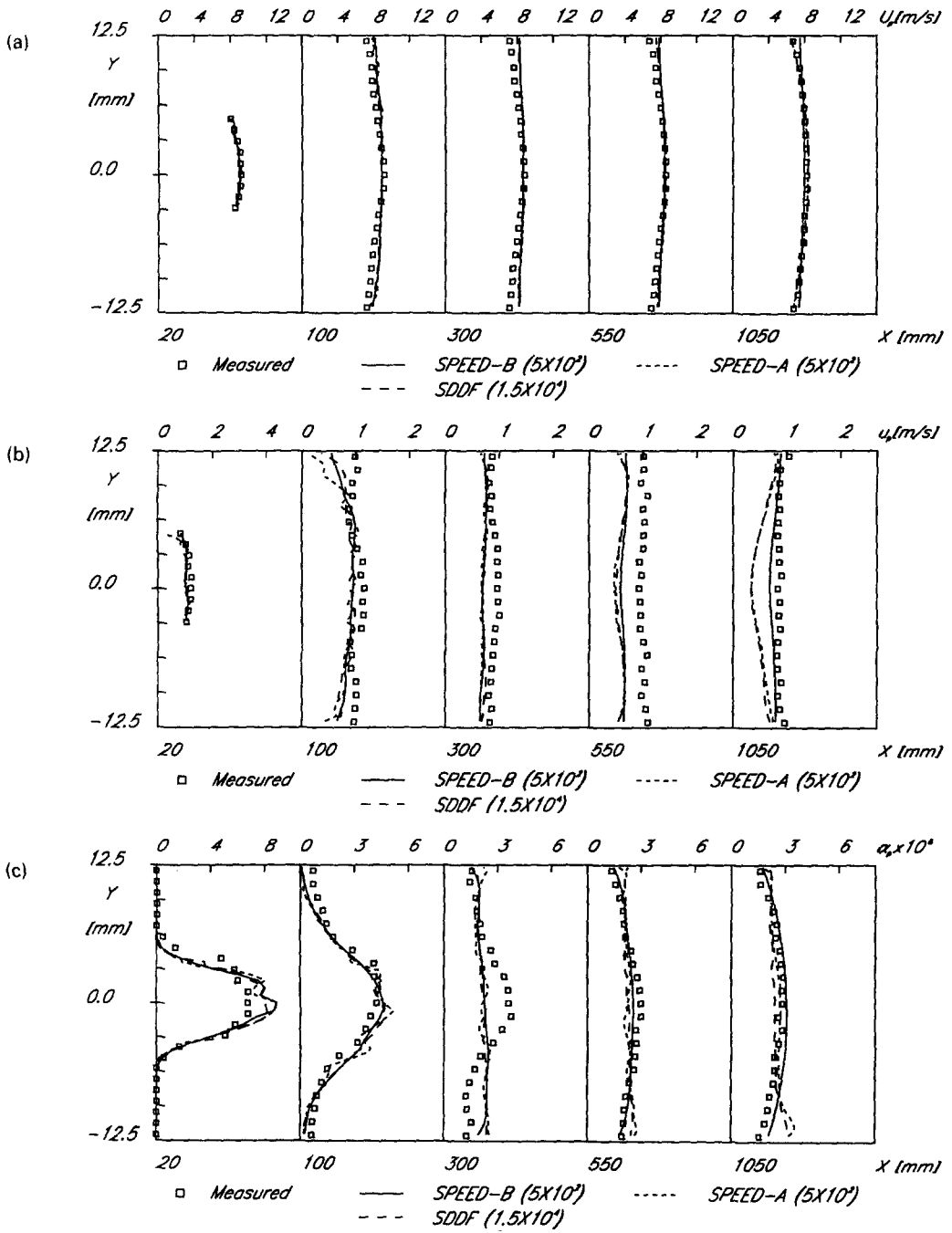

Fig. 8. Predictions of particle-phase properties with SPEED-A and SPEED-B (5×10^2) as well as SDDF (1.5×10^4): (a) axial mean velocity; (b) axial r.m.s. velocity; (c) volume concentration.

Acknowledgement—Dr Chen would like to gratefully acknowledge his post-doctoral fellowship received from the Portuguese foundation JNICT.

REFERENCES

1. Yuu, S., Yasukouchi, N., Hirosawa, Y. and Jotaki, T., Particle turbulent diffusion in dust laden round jet. *AIChE Journal*, 1978, **24,** 509–519.
2. Gosman, A. D. and Ioannides, E., Aspects of computer simulation of liquid-fuelled combustors. AIAA paper 81-0323, 1981.
3. Shuen, J.-S., Solomon, A. S. P., Zhang, Q.-F. and Faeth, G. M., Structure of particle-laden jets: measurements and predictions. *AIAA Journal*, 1985, **23,** 396–404.
4. Chang, K.-C. and Wu, W.-J., Sensitivity study on Monte-Carlo solution procedure of two-phase turbulent flows. *Numerical Heat Transfer*, 1994, **25,** 223–244.
5. Berlemont, A., Grancher, M.-S. and Gouesbet, G., Comparisons between experiments and simulations for the two-way coupling between vaporizing droplets and a turbulent round jet. *Gas-Particle Flows, ASME FED*, 1995, **228,** 279–287.
6. Fiveland, W. A. and Wessel, R. A., Numerical models for predicting performance of three-dimensional pulverized-fuel fired furnaces. *Journal of Engineering for Gas Turbines and Power*, 1988, **110,** 117–126.
7. Coimbra, C. F. M., Azevedo, J. L. T. and Carvalho, M. G., 3D numerical model for predicting NO_x emissions from an industrial pulverized coal combustor. *Fuel*, 1994, **73,** 1128–1134.
8. Faeth, G. M., Evaporation and combustion of sprays. *Progress in Energy Combustion Science*, 1983, **9,** 1–76.
9. Crowe, C. T., The state-of-the-art in the development of numerical models for dispersed phase flows. *Proceedings of International Conference on Multiphase Flows*, Tsukuba, Japan, 1991, pp. 49–59.
10. Sirignano, W. A., Fluid dynamics of sprays—1992: freeman scholar lecture. *Journal of Fluids Engineering*, 1993, **115,** 345–378.
11. Elghobashi, S., On predicting particle-laden turbulent flows. *Applied Science Research*, 1994, **52,** 309–324.
12. Sturgess, G. J., Syed, S. A. and McManus, K. R. Calculation of a hollow-cone liquid spray in uniform airstream. *Journal of Propulsion and Power*, 1985, **1,** 360–369.
13. Mostafa, A. A., Mongia, H. C., McDonnell, V. G. and Samuelsen, G. S., Evolution of particle-laden jet flows: a theoretical and experimental study, *AIAA Journal*, 1989, **27,** 167–183.
14. Chen, X.-Q. and Pereira, J. C. F., Computation of turbulent evaporating sprays with well-specified measurements: a sensitivity study on droplet properties. *International Journal of Heat and Mass Transfer*, 1996, **34,** 441–454.
15. Litchford, R. J. and Jeng, S.-M., Efficient statistical transport model for turbulent particle dispersion in sprays. *AIAA Journal*, 1991, **29,** 1443–1451.
16. Chen, X.-Q. and Pereira, J. C. F., Efficient Lagrangian stochastic transport modeling of turbulent evaporating sprays. *Proceeding of the International Symposium on Transport Phenomena in Combustion*, San Francisco, CA, 1995.
17. Rizk, M. A. and Elghobashi, S. E., A two-equation turbulence model for dispersed dilute confined two-phase flow. *International Journal of Multiphase Flow*, 1989, **15,** 119–133.
18. Adeniji-Fashola, and Chen, C. P., Modeling of confined turbulent fluid-particle flows using Eulerian and Lagrangian schemes. *International Journal of Heat and Mass Transfer*, 1990, **33,** 691–701.
19. Picart, A., Berlemont, A. and Gouesbet, G., Modeling and predicting turbulence fields and the dispersion of discrete particles transported by turbulent flows. *International Journal of Multiphase Flow*, 1986, **12,** 237–261.
20. Berlemont, A., Desjonqueres, P. and Gouesbet, G., Particle Lagrangian simulation in turbulent flows. *International Journal of Multiphase Flow*, 1990, **16,** 19–34.
21. Zhou, Q. and Leschziner, M. A., A time-correlated stochastic model for particle dispersion in anisotropic turbulence. *8th Turbulent Shear Flows Symposium*, Munich, Germany, September, 1991.
22. Chen, X.-Q. and Pereira, J. C. F., Prediction of evaporating spray in anisotropically turbulent gas flow. *Numerical Heat Transfer*, 1995, **27,** 143–162.
23. Litchford, R. J. and Jeng, S.-M., Probability density function shape sensitivity in the statistical modeling of turbulent particle dispersion. *AIAA Journal*, 1992, **30,** 2546–2549.
24. Abramowitz, M. and Stegun, I. A., *Handbook of Mathematical Functions*, Dover, New York, 1972.
25. Hishida, K., Ando, A. and Maeda, M., Experiments on particle dispersion in a turbulent mixing layer. *International Journal of Multiphase Flow*, 1992, **18,** 181–194.
26. Chen, X.-Q. and Pereira, J. C. F., Comparison of various particle dispersion models in plane mixing layer. *Numerical Methods for Multiphase Flows, ASME FED*, 1994, **185,** 217–226.
27. Crowe, C. T., Chung, J. N. and Troutt, T. R., Particle mixing in free shear flows. *Progress in Energy Combustion Science*, 1988, **14,** 171–194.
28. Azevedo, J. L. T. and Pereira, J. C. F., Prediction of gas-particle turbulent free or confined jet flows. *Particle and Particle Systems Characterization*, 1990, **7,** 171–180.
29. Chen, X.-Q. and Pereira, J. C. F., Eulerian–Eulerian predictions of dilute turbulent gas-particle flows. *Gas-Particle Flows, ASME FED*, 1995, **228,** 265–272.
30. Borner, T., Durst, F. and Manero, E., LDV measurements of gas-particle confined jet flow and digital data processing. *3rd International Symposium Applications of Laser Anemometry to Fluid Mechanics*, Lisbon, Portugal, 1986.

APPENDIX A

According to its definition, the instantaneous particle position consists of two parts:

$$x_{pi}(t) = \langle x_{pi}(t)\rangle + x'_{pi}(t) \tag{A1}$$

where the ensemble averaging has been used to denote the mean value, and the superscript represents the fluctuating value. Similarly, the instantaneous particle velocity can be written as

$$u_{pi}(t) = \langle u_{pi}(t)\rangle + u'_{pi}(t). \tag{A2}$$

On the one hand, the particle position can be computed by

$$x_{pi}(t) = \int_0^t u_{pi}(t_1)\mathrm{d}t_1 + x_{pi}(0). \tag{A3}$$

Introducing equation (A2) into equation (A3), we have

$$x_{pi}(t) = \int_0^t \langle u_{pi}(t_1)\rangle \mathrm{d}t_1 + \int_0^t u'_{pi}(t_1)\mathrm{d}t_1 + x_{pi}(0). \tag{A4}$$

On the other hand, ensemble-averaging of either side of equation (A3) yields

$$\langle x_{pi}(t)\rangle = \int_0^t \langle u_{pi}(t_1)\rangle \mathrm{d}t_1 + \langle x_{pi}(0)\rangle. \tag{A5}$$

Subtracting equation (A4) from equation (A5) and taking equation (A1) into account, we can obtain

$$x'_{pi}(t) = \int_0^t u'_{pi}(t_1)\mathrm{d}t_1 + [x_{pi}(0) - \langle x_{pi}(0)\rangle]. \quad \text{(A6)}$$

Note that each particle size issuing from the inlet represents a parcel of particles having the same initial conditions, such as diameter, velocity and position; as a result, the second term in equation (A6) diminishes. Therefore we have

$$x'_{pi}(t) = \int_0^t u'_{pi}(t_1)\mathrm{d}t_1. \quad \text{(A7)}$$